

A high excitation H II region in the faint dwarf elliptical galaxy A0951+68

R. A. Johnson^{1,2}, A. Lawrence², R. Terlevich³ and D. Carter^{3,4}

¹*Queen Mary and Westfield College, Mile End Rd., London*

²*Institute for Astronomy, University of Edinburgh, Royal Observatory, Blackford Hill, Edinburgh*

³*Royal Greenwich Observatory, Madingley Road, Cambridge*

⁴*Astrophysics Group, Liverpool John Moores University, Byrom Street, Liverpool*

2 October 2018

ABSTRACT

We present the results of BVRI imaging and optical spectroscopy of the dwarf galaxy A0951+68. The images reveal that, although this galaxy is classified as a dwarf elliptical, it has some properties that are similar to dwarf irregular galaxies. It contains two bright knots of emission, one of which is red and unresolved and the other blue and resolved. The blue knot also shows a high excitation emission line spectrum. The observed line ratios indicate that this is an H II region, although with some line ratios that are border-line with those in AGN. The emission line luminosity is consistent with ionisation by a single, very luminous O star, or several smaller O stars, but the extended blue light in the knot shows that this has occurred as part of a substantial recent star formation event. We find that the metal abundance, while low compared to typical large galaxies, actually seems to be high for such a low luminosity dwarf. The position of A0951 in the literature is incorrect and we provide the correct value.

Key words: extragalactic H II regions – dwarf irregulars and ellipticals

1 INTRODUCTION

The galaxy A0951+68 is in the Kraan-Korteweg and Tamman (KKT) catalogue of nearby galaxies (Kraan-Korteweg & Tamman 1979; Kraan-Korteweg 1986), where it is classified as a dwarf elliptical in the M81 group of galaxies. From this catalogue we have selected a complete, distance-limited subset, with a declination cut-off and excluding irregulars. A multi-wavelength survey of this subset, which includes A0951, is in progress. During the optical imaging of A0951+68, it was realised that its position in the KKT catalogue was incorrect. The source of this incorrect position was a paper by Bertola and Maffei (1974). Using the photographs presented in that paper we were able to locate and image A0951+68 at the correct position, roughly 10 arcminutes from the KKT catalogue position (see section 3). Our images showed two bright knots surrounded by low surface brightness emission. A search in the literature for objects at the new position of A0951 revealed two observations prior to those of the “discovery” of Bertola and Maffei. Karachentseva (1968) discovered the galaxy and named it Kar61. It was also contained in the list of Mailyan dwarf galaxies (Mailyan 1973) where it was called Mailyan 47.

It was no longer clear whether A0951+68 was really faint and nearby, or more distant and luminous, since the KKT distance was from an HI measurement at the incorrect position (Huchtmeier & Richter 1989). HI maps in the

literature do show emission at the correct position but it is unclear whether this is just a positional coincidence as there is extensive HI emission in the region around M81. An independent measurement of distance was required and to this end we obtained optical spectra of the two bright knots in the galaxy. One of the spectra showed very high-excitation emission lines, from which we were able to confirm that this galaxy is indeed an M81 group dwarf, but showing interesting behaviour, atypical of a dwarf elliptical. We have therefore taken the A0951 distance to be 3.63 Mpc, the same as the M81 distance (Freedman 1994).

2 OBSERVATIONS AND DATA REDUCTION

Optical images in the B,V,R and I bands were obtained using the Jacobus Kapteyn Telescope (JKT) on La Palma in February 1994. The EEV7 CCD used gives a spatial scale of 0.31 arcsec/pixel and an image size of 6'.5 × 6'.0. The seeing on this night was poor, FWHM approximately 2".0. The spectra were also taken on La Palma, in January 1995, using the Intermediate Dispersion Spectrograph (IDS) on the Isaac Newton Telescope (INT). We used a TEK CCD and the R300V grating which has a dispersion of 3.29 Å/pixel⁻¹. The FWHM of the arc lines is 8.24±0.62 Å. The slit width used was 1".5.

Table 1. Comparison of σ (arcsec) of Gaussian fits to stars and knots

	σ_{stars}	σ_{A0951A}	σ_{A0951B}
B	0.98	(1.1)	1.38
V	1.02	0.94	1.30
R	0.78	0.79	1.20
I	0.69	0.76	(0.8)

The optical images were reduced using the IRAF software package. They were debiased and flat-fielded, and calibrated using Landolt photometric standards, which give Johnson B,V and Kron-Cousins R and I magnitudes (Landolt 1983). Extinction and colour corrections were determined from these standards. The spectra were reduced using the FIGARO software package. Each object and standard frame was debiased and flatfielded, and the frames were cleaned of cosmic rays. The sky was removed from each frame by subtracting a polynomial fitted to the object free parts of each frame. 1D spectra were extracted from each frame and wavelength calibrated. The wavelength calibration was provided by Cu-Ar and Cu-Ne lamps which were observed once either side of the observations. The wavelength values we use are for standard air conditions. The wavelength scale shifted by $\approx 1\text{\AA}$ between the two lamp spectra. The average of the two wavelength scales was used to calibrate the object and standard frames that were observed between the two lamp spectra. The maximum error on the wavelength calibration is therefore $\approx 0.5\text{\AA}$. The standard and object frames were corrected for atmospheric extinction using the standard extinction curve for La Palma (King 1985) and the measurements for that night from the Carlsberg Automatic Meridian Circle. The flux standards used for the spectroscopic observations were SA 29 130 (Oke 1974) and Feige 34 (Stone 1977).

3 RESULTS

3.1 Morphology, position and colours

Figure 1 shows the R image of A0951. There are two bright knots of emission, A0951A and A0951B, superimposed on diffuse low surface brightness emission. The knot A0951A appears to be close to the peak of the diffuse emission, whereas A0951B is towards the edge of the galaxy. Figure 2 shows cuts through the galaxy and both bright knots in the sky subtracted R and B images. This also shows the central position of A0951A and highlights the difference in colour between the two knots. To see whether the two knots of emission were resolved we fitted Gaussian profiles to each knot and to three stars in each frame. Table 1 gives the average value of sigma in arcseconds for the stars and for the two knots. The brackets indicate an estimation since there was not enough signal-to-noise to enable a gaussian fit. A0951A is unresolved at all wavelengths, A0951B is clearly resolved in B,V and R.

Table 2 gives the magnitudes of the knots and the diffuse emission. To measure the knot magnitudes the images were first smoothed so that the p.s.f in each image was the same as that in the image with the worst seeing. The magnitudes for the knots were measured inside a circular aper-

Table 3. Colours

colour	Knot A	Knot B	Diffuse
B-V	0.96	0.01	0.53
V-R	0.61	0.11	0.49
V-I	0.91	-0.25	0.99

ture that enclosed all of the knot emission in all filters. The aperture radii for knot A and knot B were $3''.25$ and $4''.03$ respectively. The emission underlying each knot was found by taking the mean in an annulus surrounding the aperture and this underlying emission was subtracted from the knot magnitudes. The magnitude of the diffuse emission was found down to the surface brightness contour where the galaxy emission became indistinguishable from the sky. The surface brightness of the contour enclosing the diffuse emission is given in the table, as well as the approximate size of the galaxy down to this surface brightness. The knot magnitudes have been subtracted from the diffuse magnitude.

Table 3 gives the colours of the knots and the diffuse emission. To find the colours of the diffuse emission, its magnitude in the smoothed images was found, within a fixed area that contained significant diffuse emission in all the images.

The digitized POSS plates were used to find the RA and dec of bright stars in the optical image and from these we calculated the positions of the bright knots A0951A and A0951B to be $09^{\text{h}} 53^{\text{m}} 00^{\text{s}}.01$, $+68^{\circ} 49' 51''.3$ and $09^{\text{h}} 53^{\text{m}} 04^{\text{s}}.86$, $+68^{\circ} 50' 10''.5$ (B1950) respectively. This is ≈ 10 arcmin away from the position quoted by Bertola and Maffei (1974).

3.2 Spectrum

Figures 3 and 4 show the spectra of the two bright knots. Both spectra have featureless continua, but A0951B contains strong high excitation emission lines. The observed value of 3.19 for the Balmer decrement in A0951B is greater than the Case B recombination value of 2.86 (for $T_e=10000\text{K}$ and $N_e=100\text{ cm}^{-3}$). Using the reddening law in Savage and Mathis (1979) this implies an E(B-V) of 0.1. The galactic reddening in this direction gives an E(B-V) of 0.04 (Burstein & Heiles 1984). Table 4 lists the line identification, the observed wavelengths and the observed and de-reddened (assuming E(B-V)=0.1) line fluxes in A0951B.

To provide checks of the spectrum and image measurements, the flux of the spectra in wavelength bands roughly corresponding to the Johnson B,V and Kron-Cousins R,I filters was calculated and converted to magnitudes. Taking into account that the area of the object covered by the slit is less than the aperture used for the photometry, these magnitudes are consistent with those calculated from the images.

The strongest lines in the spectrum, H_{β} , $[\text{O III}]\lambda\lambda 4959, 5007$, and H_{α} were used to calculate the recession velocity of A0951. Applying a correction for the earth's orbit gives a heliocentric velocity of $-134.73 \pm 3.29\text{ kms}^{-1} \pm 30\text{ kms}^{-1}$. The first error here is the root mean square fitting error on the calculated velocity, the second is a systematic error due to the shift in the wavelength calibration during the night mentioned in section 2.

The measured FWHM of the H_{α} line is 9.02\AA . Recalling that the FWHM of the arc lines is $8.24 \pm 0.62\text{\AA}$, this implies

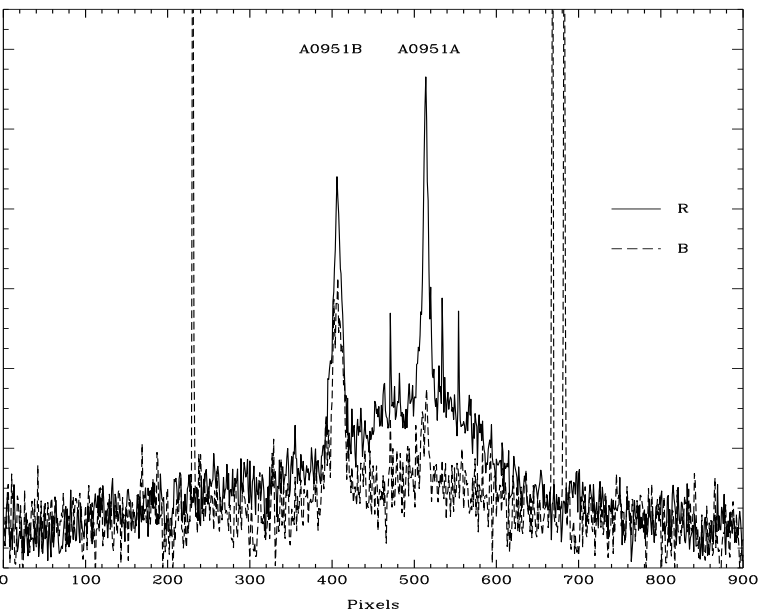


Figure 2. Cuts through the galaxy in the B and R images

Table 2. Magnitudes

filter	Knot A	Knot B	Diffuse	limiting contour mag arcsec ⁻²	approximate size (arcsec)
B	21.63	19.81	17.22	26.5	43×30
V	20.67	19.80	15.68	26.5	89×60
R	20.06	19.69	15.10	26	94×63
I	19.77	20.04	14.64	26	92×56

that the H α line is unresolved, and that, at 1σ , the intrinsic FWHM of H α < 272 km s⁻¹. This is consistent with values of < 120 km s⁻¹ found in other H II regions.

4 DISCUSSION

A0951+68 has previously been classified as a dwarf elliptical from its smooth and symmetric appearance on photographic plates. The presence of A0951B was not known and the nature of A0951A was unclear - Karachentseva et al. (1968) thought it was a foreground star, whilst Bertola & Maffei (1974) were unable to tell whether it was a star or the nucleus of the galaxy. The knot A0951A is close to the centre of the inner isophotes and this part of the galaxy has the appearance of a nucleated dwarf elliptical. However, A0951B is a high excitation H II region (see section 4.3), and this and the outer isophotes look more like an Im type irregular galaxy. In their atlas of Virgo galaxies, Sandage and Bingelli

(1984) note that there are a few cases of unsure classification between dE and Im galaxies, but are unable to say whether this is due to a real evolutionary link between the two types. The absolute V magnitude of A0951 within $\mu V = 26.5$ is -12.12. This is at the faint end of a sample of M81 dwarf irregulars observed by Miller and Hodge (1994), which have M_V between -11.9 and -16.7.

Another property of A0951 that is similar to dwarf irregulars is its probable HI content. Several groups have published maps of the neutral hydrogen emission in the vicinity of M81 which include the position of A0951 (van der Hulst 1979; Appleton et al. 1981; Yun 1994). These all show neutral hydrogen at the position of A0951. The paper by van der Hulst (1979) contains velocity channel maps which show HI at the position of A0951 with a velocity of -140 km s⁻¹, consistent with the velocity measured from our optical spectrum. However the large amount of HI in this region and the low spatial resolution of the maps means we cannot be entirely sure that the gas is coincident with A0951.

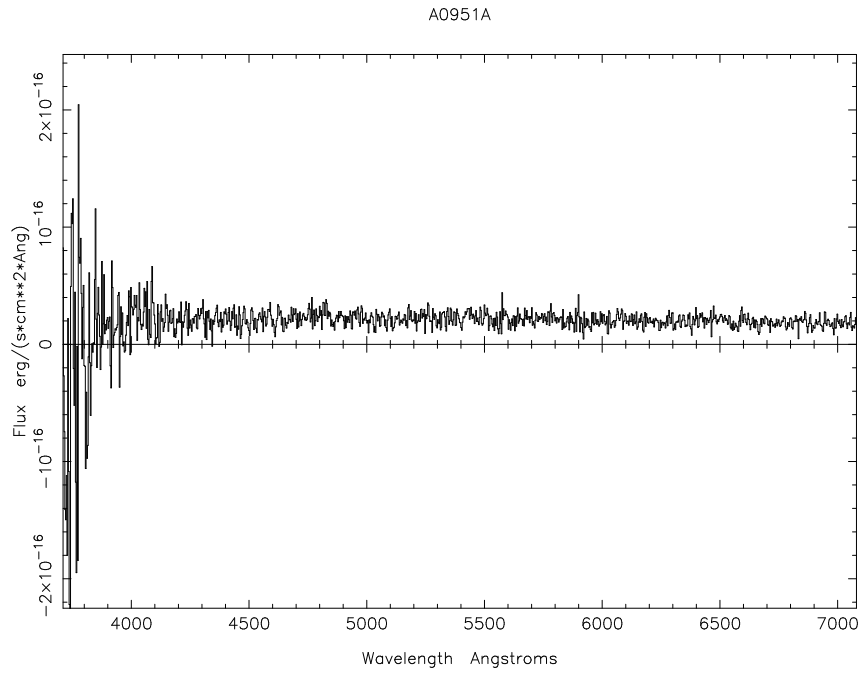


Figure 3. Spectrum of A0951A

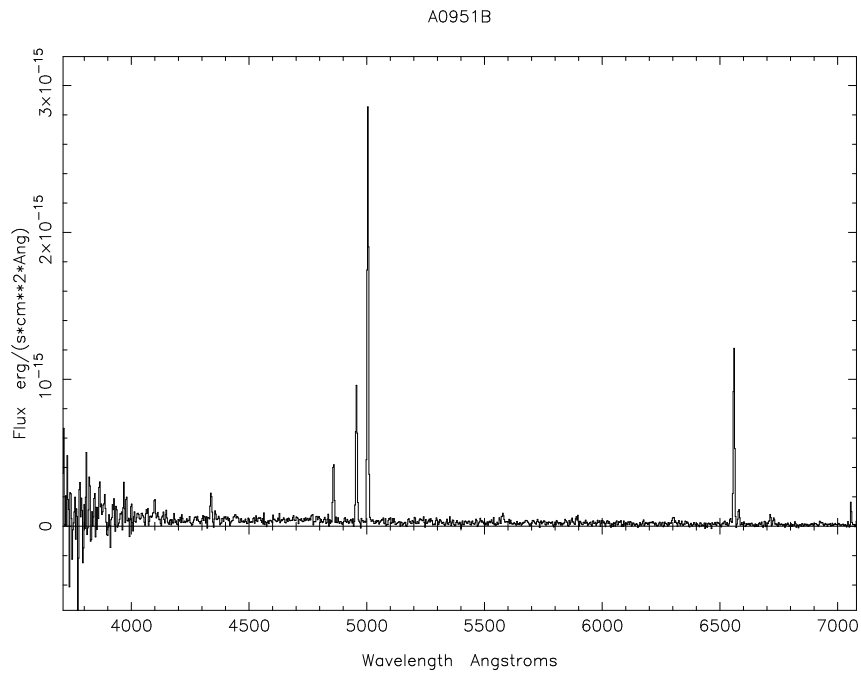


Figure 4. Spectrum of A0951B

Table 4. A0951B Line Fluxes

Line ID	λ_{obs}	$F(\lambda)/F(\text{H}\beta)_{\text{obs}}$	$F_r(\lambda)/F_r(\text{H}\beta)$
H δ 4102	4099.2	0.40	0.42
H γ 4340	4338.9	0.47	0.50
H β 4861	4858.9	1.0	1.0
[O III] 4959	4956.4	2.72	2.70
[O III] 5007	5004.5	7.75	7.68
[N II] 6548	6545.9	0.11	0.10
H α 6563	6559.7	3.19	2.86
[N II] 6584	6580.1	0.30	0.27
[S II] 6717	6713.1	0.14	0.12
[S II] 6731	6728.4	0.09	0.08
Upper limits on undetected lines			
[O II] 3727		≤ 1.38	≤ 1.52
[O III] 4363		≤ 0.17	≤ 0.18
He II 4686		≤ 0.14	≤ 0.14
[O I] 6300		≤ 0.11	≤ 0.10
Observed H β flux = 2.63×10^{-15} erg s $^{-1}$ cm $^{-2}$			
Reddening corrected H β flux = 3.71×10^{-15} erg s $^{-1}$ cm $^{-2}$			

Col 1 Line Identification, Col 2 observed wavelength

Cols 3 & 4 Observed and reddening corrected line fluxes relative to H β =1

4.1 Diffuse emission

The colours of A0951 can be used as well as the morphology to pin down its type. Figure 5 shows the colours of the two knots and the diffuse emission. The ordinate gives the colour relative to I. The positions of main sequence stars are shown, as are models of old and young stellar populations with a metallicity ($0.1Z_{\odot}$) consistent with that derived from the emission line spectrum of knot B (see section 4.3). The 8Gyr model is from Worthey (1994) and fits well the colours of the diffuse emission and of knot A. A slightly better fit is provided assuming a metallicity of $0.03Z_{\odot}$, but this is lower than found from the emission lines. The colours of the diffuse emission are very similar to those of a G star. The B-V colour of 0.53 of the diffuse emission is bluer than that of dwarf ellipticals in the Virgo and Fornax clusters (Caldwell 1983; Caldwell & Bothun 1987) which have a mean B-V of 0.78. Gallagher and Hunter (1987) present colour-colour diagrams in BVRI for a sample of irregular and amorphous galaxies, and A0951 has the same position on these diagrams as these galaxies. Although these galaxies are more luminous than A0951, the colours of dwarf irregulars are similar as indicated by the mean B-V colour of 0.47 of dwarf irregulars in Virgo (Bothun et al. 1986), and a mean B-V of 0.37 in a sample of dwarf irregulars also observed by Hunter and Gallagher (1985).

4.2 A0951A

Knot A has much redder colours than Knot B. The V-I colour is similar to that of the diffuse emission; the other colours are somewhat redder. As we do not have a redshift for this knot there is the possibility that it is a superimposed foreground star - in Figure 5 it can be seen that the colours of A0951A are closest to those of a G star. The B-V colour of A0951A is at the far red end of the colours of dwarf ellipticals in the Virgo and Fornax clusters. The B-V, V-R

and R-I colours of A0951A are similar to those in a sample of low luminosity early type galaxies observed by Prugniel et al (1993). Some dwarf ellipticals are nucleated and these nuclei have similar colours to the surrounding emission. The colours and morphology of A0951A are reminiscent of these dwarf elliptical nuclei.

The spectrum of A0951A is flat and featureless. Held and Mould (1994) show spectra of dwarf elliptical nuclei. On the whole they are not as flat as A0951A. The most prominent feature in these spectra is the 4000Å break, unfortunately at this wavelength the spectrum of A0951A has very low signal to noise and although there is a hint of a break it is impossible to say whether it is real. The signal to noise in our spectrum is too low to observe the absorption features seen in these spectra.

4.3 A0951B

The spectrum of A0951B is very striking. The value of the [O III] λ 5007/H β λ 4861 ratio is as high as that seen in active galaxies, but the [N II] λ 6584/H α 6563 ratio is much lower, suggesting low metallicity. The different types of emission line object, H II regions and galaxies, active galaxies and planetary nebulae can be separated by their positions on emission line ratio diagrams such as those of Veilleux and Osterbrock (1987) and Baldwin, Phillips and Terlevich (1981). In these diagrams A0951 occupies the area populated by H II regions and H II galaxies, though the [O III] λ 5007/H β λ 4861 ratio in this galaxy is amongst the highest seen. A0951B is somewhat peculiar in that the few other H II galaxies and regions that have a similar [O III] λ 5007/H β λ 4861 ratio have even lower [N II] λ 6584/H α 6563 ratios. The value of [N II] λ 6584/H α 6563 in A0951B puts it in the transition region between H II regions and AGN. Also (see below), although its metal content is low compared to typical large galaxies, it is actually high compared to other H II galaxies of the same luminosity.

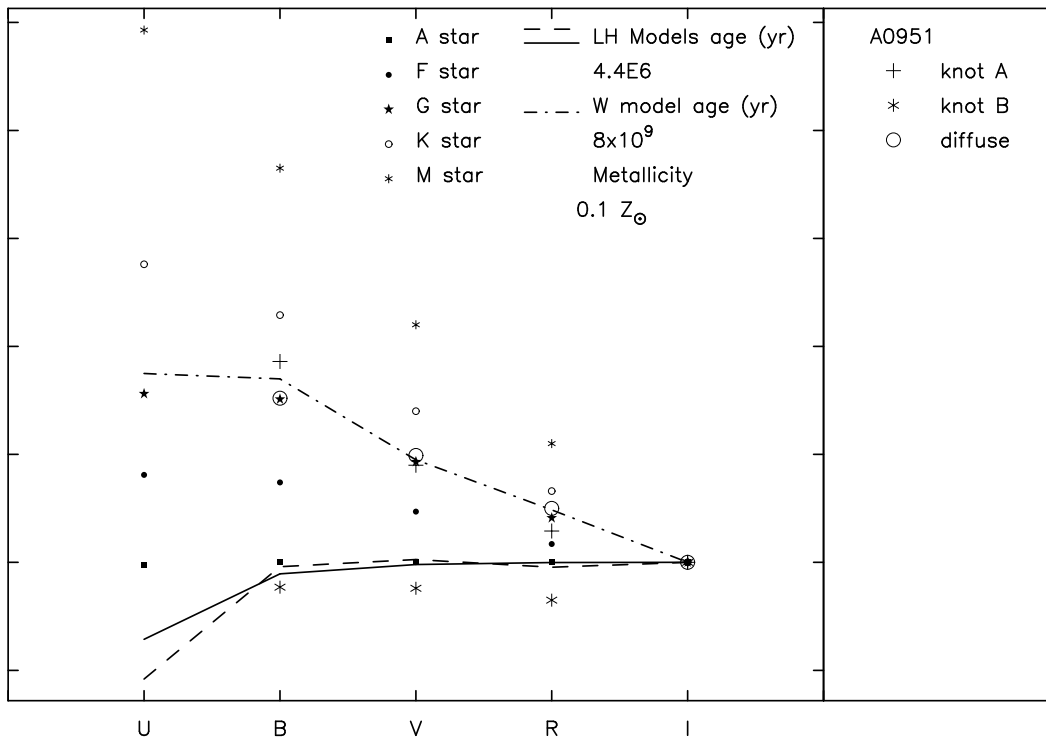


Figure 5. Colour of A0951 knots and diffuse emission. The ordinate is the colour relative to I, i. e. at B the value is B-I. The stellar population models are those in Worthey (1994) and Leitherer & Heckman (1995) (see sections 4.1 and 4.3). Both models are low metallicity, $0.1Z_{\odot}$

The observed emission line ratios in H II regions depend upon the properties of the ionized gas and on the ionizing stars. Some of these properties can be calculated directly from the observations, others can be found by comparing the observations with models of H II regions.

From the observed emission lines in A0951B we can deduce the electron temperature and density of the gas, and the number of ionizing photons. The electron temperature in the O^{++} region can be found from the ratio of the $[O\text{III}]\lambda\lambda 4959, 5007$ doublet and $[O\text{III}]\lambda 4363$. The fluxes in table 4 give an upper limit to the temperature of 15500 K. The electron density can be estimated from the $[S\text{II}]\lambda\lambda 6717, 6731$ doublet; however this loses sensitivity at typical H II galaxy densities of less than $\approx 200\text{ cm}^{-3}$. The density in A0951B is in this low density limit. The number of hydrogen ionizing photons, $Q(H)$, emitted by the ionizing stars is given by the relationship $Q(H)(\text{s}^{-1}) = 7.31 \times 10^{11} L_{H\alpha}(\text{ergs}^{-1})$ (Osterbrock 1989). Using the reddening corrected $H\alpha$ luminosity for A0951B gives $Q(H) = 1.20 \times 10^{49}\text{ s}^{-1}$. This number of ionizing photons could be produced by one star of spectral type O7 ($T_e=45200\text{ K}$) or several stars of later type.

Two of the most recent H II region models are those of Cervino and Mas-Hesse (1994) and García-Vargas, Bressan and Díaz (1995). Both these models vary the ionization parameter, the effective temperature of the ionizing cluster (T_e), and the metallicity of the gas, and calculate the emission line ratios produced. The ionization parameter, U , is defined as the ratio between the density of the ionizing photons and the density of particles ($U = Q(H)/4\pi cn_H r^2$), where n_H is the density of ionized hydrogen). This depends on the number of ionizing photons, the density of hydrogen atoms and the radius of the H II region, so knowing the first two of these parameters would enable us to estimate the radius of the H II region. In fact we only have an upper limit on the density, but the interesting thing to work out is how the radius of the H II region compares to the Stromgren radius, and the ratio of these two radii only depends upon $(\text{density})^{1/6}$.

The aim of Cervino and Mas-Hesse was to calculate the dependence of the most commonly observed emission lines, those of oxygen, on these parameters. From our limits on the oxygen emission line ratios in A0951 we can deduce from their models that T_e is between 45000 and 55000 K and the

oxygen abundance, $\log(\text{O}/\text{H})$, between -4.2 (1/12 solar) and -3.8 (1/5 solar). They do not say what value of ionization parameter they use. They show the parameters derived from their models for a sample of H II galaxies (Terlevich 1991). Comparison of A0951B with these galaxies shows that it has a similar metal content to the average H II galaxy, but a much lower luminosity.

García-Vargas et al. model the behaviour of more emission lines, and look at the line ratios for different ages of the ionizing star cluster (and hence different T_e) and for varying metallicity and ionization parameter. Their models suggest that A0951 has a metallicity, Z , between 0.001 (1/17 Z_\odot) and 0.008 (1/2 Z_\odot), an age between 2 and 5.2 Myrs (implying a T_e between 40000 and 50000K), and an ionization parameter, $\log U$, between -2.7 and -2.4. From this we can deduce that the radius of the H II region is the same as the radius of a Strömgren sphere of an O7 star. The range of effective temperatures implied by these models, combined with the number of ionizing photons is consistent with ionization by a single such O star, or a few, later-type O stars.

It is interesting to compare A0951 with GR8, a dwarf irregular in the local group (Skillman et al. 1988). While their total absolute magnitudes (-12.1 and -10.7) and H II region luminosities ($L(\text{H}\beta)$ 1.4×10^{36} and 5.8×10^{36}) are comparable, the metal content of A0951 seems to be much higher than that of GR8 or other star forming regions of the same total luminosity. This may suggest a different chemical evolution history for A0951, perhaps related to the fact that A0951 is not a dwarf irregular. Clearly a better estimate of the metal abundances is needed.

The $\text{H}\alpha$ luminosity of A0951B is 1.64×10^{37} ergs s^{-1} . This is at the low end of the range of luminosities seen in dwarf irregulars. It is interesting to note that one of the dwarf irregular H II regions observed by Hunter and Gallagher (1985) has an ionizing source of a single O star, and similar line ratios to A0951B with $[\text{O III}]\lambda 5007/\text{H}\beta\lambda 4861 = 6.18$. The $\text{H}\beta$ equivalent width in A0951B is 92.8 Å which is higher than the mean equivalent width in the Terlevich et al. (1991) sample of H II galaxies and is indicative of a young stellar population.

The emission-line region that we have been discussing occurs somewhere inside the resolved blue knot A0951B, which is clearly much bigger and more luminous than a single O star. The colours of knot A0951B are similar to those in resolved regions of star formation found in some Virgo dwarf irregulars by Bothun et al. (1986). A recent paper by Leitherer & Heckman (1995) shows the change in colours of a model starburst galaxy with metallicity and age. Their model for a metallicity of 0.1 Z_\odot and an age of 4.4 Myr (chosen to be consistent with the values deduced from the spectrum) is shown in Figure 5. The solid line is for an instantaneous burst and the dashed line for continuous star formation. It can be seen that the model colours are reasonably similar to the colours of A0951B. We conclude that A0951B is a region of very recent star formation which in particular contains an H II region ionized by at most a few O stars, with an effective temperature of around 45000-50000K.

5 CONCLUSIONS

Optical images and spectroscopy of the M81 dwarf A0951+68 have provided a few surprises, not least that the published position of the galaxy was incorrect. We have calculated a new position. Another surprise was the presence in this supposed dwarf elliptical galaxy of an H II region, with very high excitation. H II region models suggest that the ionizing source is a single very luminous O7 star, or a few later-type O stars. The colours of the knot A0951B, which contains this H II region, are consistent with it being a star formation region. The colours of the diffuse emission in A0951, the presence of the star forming region and also the fact that it probably contains H I gas make A0951 more like a dwarf irregular than a dwarf elliptical. However, the knot of emission at the centre of the inner isophotes (A0951A) has colours that are similar to those of low luminosity ellipticals and is reminiscent of the nuclei seen in some dwarf elliptical galaxies.

ACKNOWLEDGEMENTS

The Jacobus Kapteyn and Isaac Newton telescopes are operated on the island of La Palma by the Royal Greenwich Observatory in the Spanish Observatorio del Roque de los Muchachos of the Institute de Astrofísica de Canarias. The IRAF and FIGARO software packages used to reduce the data are distributed by NOAO and Starlink respectively. RAJ acknowledges receipt of a PPARC studentship.

REFERENCES

- Appleton P.N., Davies R.D., Stephenson R.J., 1981, MNRAS, 195, 327
 Baldwin J.A., Phillips M.M., Terlevich R., 1981, PASP, 93, 5
 Bertola F., Maffei P., 1974, A&A, 32, 117
 Börngen F., Karachentseva V.E., Schmidt R., Richter G.M., Thänert W., 1982, Astr. Nachr., 303, 287
 Bothun G.D., Mould J.R., Caldwell N., MacGillivray H.T., 1986, AJ, 92, 1007
 Burstein D., Heiles C., 1984, ApJS, 54, 33
 Caldwell N., 1983, AJ, 88, 804
 Caldwell N., Bothun G.D., 1987, AJ, 94, 1126
 Cerviño M., Mas-Hesse J.M., 1994, A&A, 284, 749
 Chaboyer B., 1993, "Dwarf Galaxies" ESO/OHP workshop, 485
 Freedman W.L. et al., 1994, ApJ, 427, 628
 Gallagher III J.S., Hunter D.A., 1987, AJ, 94, 43
 García-Vargas M.L., Bressan A., Díaz A.I., 1995, A&AS, 112, 13
 Held E.V., Mould J.R., 1994, AJ, 107, 1307
 Huchtmeier W.K., Richter O.G., 1989, A general catalog of HI observations of galaxies, Springer-Verlag, New York
 Hunter D.A., Gallagher III J.S., 1985, ApJS, 58, 533
 Karachentseva V.E., 1968, Soobsch. Byurakan Observatory, 39, 61
 Karachentseva V.E., Karachentsev I.D., Börngen F.B., 1985, A&AS, 60, 213
 Kennicutt R., 1983, ApJ, 272, 54
 King D.L., 1985, La Palma Technical Note 4
 Kraan-Korteweg R.C., Tamman G.A., 1979, Astr. Nachr., 300, 181
 Kraan-Korteweg R.C., 1986, A&AS, 66, 255
 Landolt A.U., 1983, AJ, 88, 439
 Leitherer C., Heckman T.M., 1995, ApJS, 96, 9
 Madore B.F., 1994, PASP, 106, 63

- Mailyan N.S. 1973, *Astrofizika*, 9, 33
Miller B.W., Hodge P., 1994, *ApJ*, 427, 656
Oke J.B., 1974, *ApJS*, 27, 21
Osterbrock D.E., 1989, *Astrophysics of Gaseous Nebulae and Active Galactic Nuclei*
Prugniel P., Bica E., Klotz A. and Alloin D., 1993, *A&AS*, 98, 229
Sandage A., Bingelli B., 1984, *AJ*, 89, 919
Savage B.D., Mathis J.S., 1979, *Ann. Rev. Astr. Ast*, 17, 73
Skillman E.D., Melnick J., Terlevich R., Moles M., 1988, *A&A*, 196, 31
Stone R.P.S., 1977, *ApJ*, 218, 767
Terlevich R., Melnick J., Masegosa J., Moles M., Copetti M.V.F., 1991, *A&AS*, 91, 285
Worthey G., 1994, *ApJS*, 95, 107
van der Hulst J.M., 1979, *A&A*, 75, 97
Veilleux S., Osterbrock D.E., 1987, *ApJS*, 63, 295
Yun M.S., Ho P.T.P., Lo K.Y., 1994, *Nature*, 372, 530

This figure "figure1.jpg" is available in "jpg" format from:

<http://arxiv.org/ps/astro-ph/9702217v1>